Synthesis and Characterization of Halogenated Amorphous Silicon via a Novel Glow Discharge Process

Oscar H. Giraldo,[†] William S. Willis,[†] Manuel Márquez,[†] Steven L. Suib,[*,†,‡] Yuji Hayashi,[†] and Hiroshige Matsumoto[†]

U-60, Department of Chemistry, and Department of Chemical Engineering, University of Connecticut, Storrs, Connecticut 06269-4060

Received July 29, 1997. Revised Manuscript Received November 12, 1997

Amorphous silicon powder has been produced in a tubular glow discharge reactor. Reaction were done using $SiCl_4$ discharges of a mixture of hydrogen and helium at atmospheric pressure. Chemical and physical characterization of the product shows that about 1% Cl is present, the powders are predominantly amorphous, semiconducting behavior is observed, and surface oxidation occurs due to exposure to moist air. The bandgap of the material before prolonged air exposure measured by diffuse reflectance ultraviolet−visible spectroscopy methods is between 2.4 and 2.6 eV.

Introduction

The use of plasmas to prepare powdered materials is an area of considerable recent interest such as in the preparation of diamond particles and coatings.[1] The advantages of cold plasmas, which are those that have considerably different thermal and electronic temperatures, are fundamentally related to the ability to operate under conditions where local thermodynamic equilibria do not exist.[2] Such plasmas avoid the exposure of the reactant walls, reagents, and products to excessively high temperatures that can cause sintering, crystal growth, phase changes, melting, and other potentially undesirable processes.

Several types of plasmas can be used to prepare materials and to treat surfaces. Some commonly used plasmas include microwave plasmas,[3] radio frequency plasmas,[4] corona discharges,[5] and glow discharges.[6] Each of these different types of plasmas has potential advantages and disadvantages for the production of new materials including the temperatures (thermal and electronic),[7] apparatus, energy requirements, power supplies, pressures, and atmospheres that can be used.

Silicon is one of the most important semiconductor materials. Silicon is used in photoelectric applications,[8,9] and its properties are markedly influenced by methods of synthesis used in preparation. Hydrogenated amorphous silicon has been produced in glow discharges of silane, disilane, silane/H_2 mixtures, and silane/noble gas mixtures.[10−12] Recent interest in halogenated and hydrogenated Si films (Si;H,Cl and Si;H,F) is related to the possibility for use in low-cost photovoltaic devices.[13−17]

In this research we report the use of tubular glow discharges that are operated in an ac mode at atmospheric pressure. Our goal has been to prepare new materials that are silicon based with such systems. The reaction reported here is that of $SiCl_4$ with H_2/He mixtures. Amorphous silicon materials are some of the materials that we have encountered in such studies. This paper reports the synthesis and characterization of such systems.

Experimental Section

Reagents. A gas mixture of 6% H_2 in He was prepared and used to transport $SiCl_4$ from a bubbler into the reactor.[18] $SiCl_4$ was purchased from Alfa Chemical Co., Danvers, MA. The $SiCl_4$ was transferred in a glovebag to a bubbler that had shutoff valves on each end for storage under an inert gas

* To whom correspondence should be addressed.
† Department of Chemistry.
‡ Department of Chemical Engineering.

(1) (a) Capitelli, M.; Colonna, G.; Hassouni, K.; Gicquel, A. *Plasma Chem. Plasma Processing* **1996**, *16*, 153−171. (b) Ohl, A. *Pure Appl. Chem.* **1994**, *66*, 1397−1404.
(2) (a) Fridman, A. A.; Rusanov, V. D. *Pure Appl. Chem.* **1994**, *66*, 1267−1274. (b) Inomota, K.; Koinuma, H.; Oikawa, Y.; Shiraishi, T. *Appl. Phys. Lett.* **1995**, *66*, 2188−2190.
(3) Huang J.; Suib, S. L. *J. Phys. Chem.* **1993**, *97*, 9403−9407.
(4) d'Agostini, R.; Capezzuto, P.; Bruno, G.; Cramarossa, F. *Pure Appl. Chem.* **1985**, *57*, 1287−1298.
(5) Penetrante, B. M.; Hsiao, M. C.; Bardsley, J. N.; Merritt, B. T.; Vogtlin, G. E.; Wallman, P. H.; Kuthi, A.; Burkhart, C. P.; Bayless, J. R. *Pure Appl. Chem.* **1996**, *68*, 1083−1087.
(6) Bertran, E.; Costa, J.; Viera, G.; Zhang, Q. *J. Vac. Sci. Technol. A* **1996**, *14*, 567−571.
(7) Kampas, F. J. *J. Appl. Phys.* **1983**, *54*, 2276−2280.
(8) (a) Brodsky, M. H. *Thin Solid Films* **1977**, *40*, L23−25. (b) Brodsky, M. H. *Thin Solid Films* **1978**, *50*, 57−67.
(9) (a) Yonezawa, F. *Science* **1993**, *260*, 635−640. Borman, S. *Chem. Eng. News* **1994**, *72*, No. 4, 7−8. Sakai, H. *Solar Energy Mater. Solar Cells* **1994**, *34*, 9−17. Wagner, H. *Phys. Status Solidi B, Bas. Res.* **1995**, *192*, 29−239.
(10) Perrin, J. *J. Non-Cryst. Solids* **1991**, *137−8*, 639−644.
(11) Gates, S. M. *Chem. Rev.* **1996**, *96*, 1519−1532.
(12) Jainsky, J. M.; Gates, S. M. *Acc. Chem. Res.* **1991**, *24*, 9−15.
(13) Matsumara, H.; Nakagome, Y.; Furukawa, S. *Appl. Phys. Lett.* **1980**, *36*, 439−440.
(14) Bruno, G.; Capezzuto, P.; Cramarossa, F. *Thin Solid Films* **1983**, *106*, 145−152.
(15) Bruno, G.; Capezzuto, P.; Cramarossa, F.; d'Agostini, R. *Thin Solid Films* **1980**, *67*, 103−107.
(16) Iqbal, Z.; Capezzuto, P.; Braun, M.; Oswald, H. R.; Veprek, S.; Bruno, G.; Cramarossa, F.; Stüssi, H.; Brunner, I.; Schärli, M. *Thin Solid Films* **1982**, *87*, 43−51.
(17) Mayo, N.; Carmi, U.; Rosenthal, I.; Ani, R.; Manory, R.; Grill, A. *J. Appl. Phys.* **1984**, *55*, 4404−4411.
(18) Kmetz, M. A.; Suib, S. L.; Galasso, F. S. *J. Am. Ceram. Soc.* **1990**, *73*, 3091−1093.

S0897-4756(97)00536-X CCC: $15.00 © 1998 American Chemical Society
Published on Web 01/01/1998

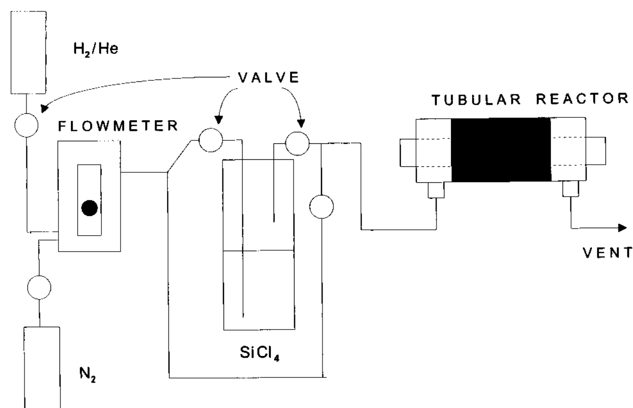

Figure 1. Diagram of tubular reactor used for glow discharge experiments.

atmosphere. A separate N_2 gas flow was used for purging the reactor prior to and after use.

Glow Discharge Apparatus. The apparatus consisted of gas mixtures of 6% H_2 in He and N_2, a flow meter, a bubbler and bypass, and a tubular reactor. A gas flow rate of 22 mL/min was used. The tubular reactor consisted of an inner stainless steel electrode (o.d. = 8 mm) in a hollow quartz tube (i.d. = 10 mm, o.d. = 12 mm) of 9 in. length. The outer copper foil electrode was wrapped around the outside of the quartz tube and held in place with copper wire. Both electrodes were connected to an Inter high-frequency power supply that was operated at 8.117 kHz with a voltage applied to the electrodes of 1.4 kV. The ac experiments were monitored with a digital oscilloscope Model DL1540 from Yokogawa, attached to a Tektronix Model P6015A high-voltage probe. The effluent was vented to a hood. The solid product was an off white or cream color. The time of reaction was typically 9 h. A diagram of the apparatus is shown in Figure 1.

Characterization Studies. *1. Fourier Transform Infrared Spectroscopy.* Diffuse reflectance Fourier transform infrared (DRIFTS) spectroscopy was used to characterize the solid product. The spectrometer was Nicolet Magna Model 750. Midinfrared spectra were collected between 4000 and 500 cm^{-1}.

2. Scanning Electron Microscopy and Energy-Dispersive X-ray Analysis. Scanning electron microscopy (SEM) and energy-dispersive X-ray (EDX) analyses were done to determine the morphologies of the samples and their elemental compositions, respectively. An AMRAY Model 1410D SEM was used at 16.0 kV for morphological experiments and 25 kV for EDX experiments. Samples were loaded onto a Cu grid and uncoated for analyses. The reproducibility of elemental analyses from EDX are within about 5%.

3. Thermogravimetric Analyses and Differential Scanning Calorimetry. Thermogravimetric analyses (TGA) and differential scanning calorimetry (DSC) experiments were done on a Perkin-Elmer Series 7 thermal analyzer instrument. About 4 mg samples were used for the DSC experiments in an O_2 gas flow at atmospheric pressure from room temperature to 800 °C at a heating rate of 10 °C/min. Similar conditions were used for the DSC experiments except 1 mg samples were used.

4. Scanning Auger Microscopy. Scanning Auger microscopy (SAM) experiments were done on a Physical Electronics, Inc. A PHI Model 610 spectrometer at a base pressure of 5×10^{-9} Torr. A single-pass cylindrical mirror analyzer with a coaxial electron gun was used, and spectra were recorded with an energy resolution of 0.6%. A beam voltage of 2 kV, a time per step of 50 ms, and 100 sweeps were used to collect the data. The sample powder was pressed into In foil for analysis. The reproducibility of the surface analyses where elemental surface concentrations are determined is generally within about 10%.

5. Diffuse Reflectance Ultraviolet–Visible Spectroscopy. Diffuse reflectance ultraviolet–visible (DRUV–Vis) spectroscopy experiments were done with a Hewlett-Packard 8452A diode array spectrophotometer equipped with a Labsphere RSA-HP-84 reflectance accessory. Samples were diluted with $BaSO_4$ for analysis and the scan range was 200–800 nm. All experiments were done at room temperature.

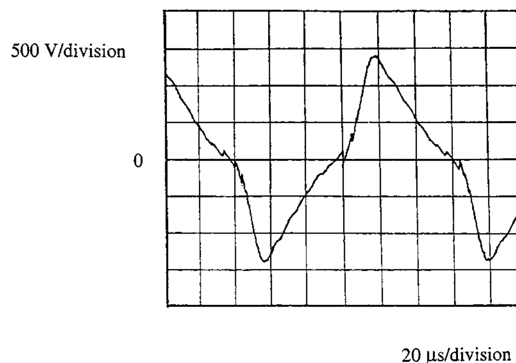

Figure 2. Plot of current versus voltage waveform for the glow discharge.

6. X-ray Powder Diffraction. X-ray powder diffraction (XRD) experiments were done with a Scintag Model XDS 2000 diffractometer with a Cu Kα radiation source. The X-ray tube was operated at 45 kV and at a current of 40 mA. Powders were sprinkled onto an aluminum sample holder.

Results

Glow Discharge Apparatus. The ac glow discharge experiments showed a uniform glow throughout the tubular reactor. The color of the glow was purple. An example of the current–voltage waveform recorded with a digital oscilloscope is shown in Figure 2. The maximum current value represents the breakdown voltage in the discharge for data of Figure 2. The oscillations after the breakdown voltage represent the glow discharge regime which lasts on the order of a few microseconds. This specific waveform is representative of waveforms collected during the 9 h experimental period. No significant changes in waveform were observed during the experiments.

The inside of the reactor developed a coating of solid particulates having an off-white or cream color during the experiments. The powder did not adhere to the walls of either the quartz reactor or the stainless steel electrode after the experiment and was readily removed by gently tapping the end of the tube or with a spatula. About 0.1 g of product was obtained.

Characterization Studies. *1. Fourier Transform Infrared Spectroscopy.* A Fourier transform infrared spectrum between 2300 and 2000 cm^{-1} of the solid product is given in Figure 3. Two major bands are observed at 2251 and 2135 cm^{-1}. The low-frequency band is broader than the higher frequency band.

Comparative DRIFTS spectra for the solid product before and after exposure to water vapor are shown in Figure 4a,b, respectively. The bands at 2251 and 2135 cm^{-1} have changed their relative intensity after exposure to water vapor. A broad very intense band centered at 3300 cm^{-1} is also observed on exposure to water vapor.

2. Scanning Electron Microscopy and Energy-Dispersive X-ray Analysis. Scanning electron microscopy data show that the solid particulates consist of aggregates on the order of 100 Å, which appear to be made up of particulates that are <5 m. Energy-dispersive X-ray analyses show that only two elements are detected, Si

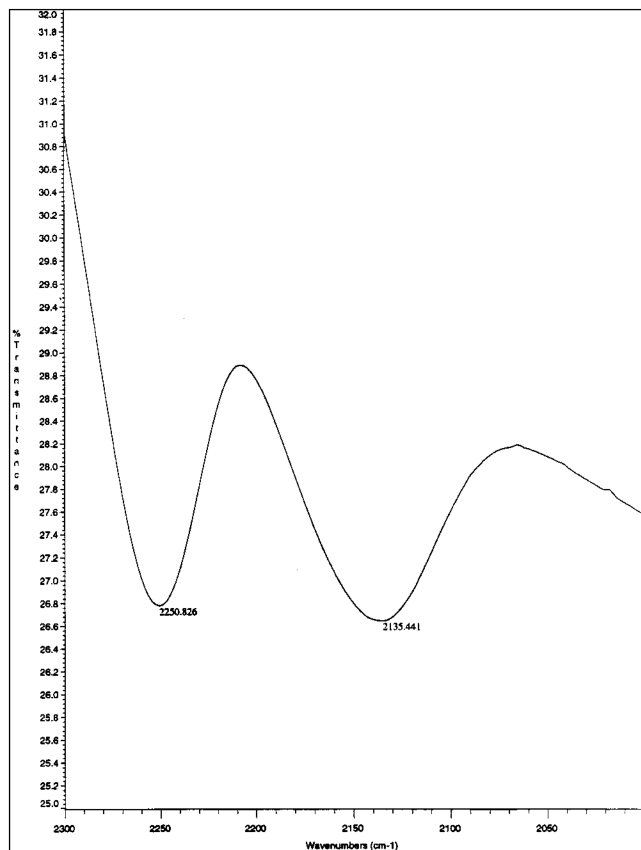

Figure 3. Fourier transform infrared spectrum of solid product.

and Cl. The Cl is at a level of <2 wt %. Such analyses represent bulk analyses in a 2 m depth.

3. Thermogravimetric Analyses and Differential Scanning Calorimetry. Thermogravimetric analytical data for the solid product are shown in Figure 5. These TGA data are for a sample heated at 10 °C/min in pure O_2. Note that there is an overall loss of about 15% up to about 200 °C. Above 200 °C there is a gain of about 5 wt %. When experiments are done in a N_2 atmosphere instead of oxygen, the total weight loss is about 16% with a very broad temperature regime where there is no weight loss, followed by a weight gain of about 7% starting at 400 °C and leveling off at about 800 °C.

Differential scanning calorimetry data for the solid product heated at 10 °C/min in N_2 is shown in Figure 6. An endothermic transition occurs around 100 °C and an exothermic transition at 195 °C. Two more endothermic transitions occur near 250 and 400 °C with another exothermic transition occurring near 350 °C.

A DRIFTS spectrum for the solid product that was heated in the TGA experiment of Figure 5 is shown in Figure 7. Note that there are several relatively sharp but weak transitions between 4000 and 2700 cm^{-1} and that the bands originally present at 2251 and 2135 cm^{-1} (Figure 3) are no longer present.

4. Scanning Auger Microscopy. Scanning Auger microscopy data for the solid product are shown in Figure 8. Peaks at 63, 78, 182, and 271 eV and 466, 487, and 509 eV are observed which are assigned to Si, Cl, C, and O, respectively. Other transitions Si (KLL) are also observed at 1603 and 1605 eV. Extra peaks in the spectrum of Figure 8 at 296 and 344 eV are due to the In MNN transition and at 398 and 403 eV for the In MNN derivative peaks since In foil was used as a sample holder. The relative intensities of each of these peaks is 63% Si, 1.0% Cl, 25.2% C, and 12.4% O. These data are semiquantitative at best with ratios of elements being most informative. These data can also be influenced by adsorbed adventitious hydrocarbons and surface oxidation.

5. Diffuse Reflectance Ultraviolet–Visible Spectroscopy. Diffuse reflectance ultraviolet–visible spectroscopy data for the solid product are shown in Figure 9. These DRUV–vis data show a broad band centered near 380 nm which tails to about 500 nm.

6. X-ray Powder Diffraction. X-ray powder diffraction data for the solid product are shown in Figure 10. The data of Figure 10 show a broad intense peak centered at about 25° 2θ with several other sharper peaks of lower intensity superimposed on the broad peak which are centered at 3.880, 2.739, 2.231, 1.99, 1.733, and 1.584 Å.

Discussion

Characterization of Amorphous Silicon. *1. Surface Functional Groups.* The DRIFTS data of Figure 3 are indicative of SiH_2 and SiH functional groups.[15,16] Bands at 2090 and 2230 cm^{-1} have been assigned to SiH_2 and SiH functional groups,[8,15,16] respectively, in hydrogenated amorphous silicon. The relative intensities of these two bands and the observed peak widths are virtually identical with materials reported by both Bruno et al.[15] and Brodsky.[8] Further support for these assignments comes from the research of Ouwens et al.[27]

DRIFTS data outside this region of the mid-infrared shown in Figure 4a show broad absorption for OH groups in the material before exposure to moist air. After exposure to moist air over a 2 week period, the broad band centered at 3300 cm^{-1} due to OH groups has markedly increased in intensity, as shown in Figure 4b. In addition note that the relative intensities of the bands at 2251 and 2135 cm^{-1} have significantly changed with the band at 2135 cm^{-1} being more intense, suggesting a change from SiH_2 groups to SiH groups in the sample exposed to moist air.[8,15,16]

These DRIFTS data are indicative of interaction of an air-sensitive surface on exposure to moist air. The data are in line with defect surface groups of a material like amorphous silicon undergoing reaction in time.

(19) Augelli, V.; Murri, R.; Schiavulli, L.; Bruno, G.; Capezzuto, P.; Cramarossa, F.; Evangelisti, F.; Fortunato, G. *Thin Solid Films* **1981**, *86*, 359–367.
(20) Veprek, S.; Iqbal, Z.; Oswald, H. R.; Webb, A. P. *J. Phys. C: Solid State Phys.* **1981**, *14*, 295–308.
(21) (a) de Ruiter, R.; Jansen, J. C.; van Bekkum, H. In *Molecular Sieves*; Occelli, M. L., Robson, H., Eds.; Van Nostrand Reinhold: New York; pp 167–189. (b) Xu, W. Q.; Yin, Y. G.; Suib, S. L.; O'Young, C. L. *J. Catal.* **1994**, *150*, 34–45.
(22) Hwan, L.; Willis, W. S.; Galasso, F. S.; Suib, S. L. *Adv. Ceram. Mater.* **1988**, *3*, 584–589.
(23) Buss, R. J.; Babu, S. V. *J. Vac. Sci. Technol. A* **1996**, *14*, 577–581.
(24) Ho, P.; Buss, R. J.; Loehman, R. E. *J. Mater. Res.* **1989**, *4*, 873–881.
(25) Walkup, R.; Avouris, Ph.; Dreyfus, R. W.; Jasinski, J. M.; Selwyn, G. S. *Appl. Phys. Lett.* **1984**, *45*, 372–374.
(26) Perrin, J.; Schmitt, J. P. M. *Chem. Phys.* **1982**, *67*, 167–176.
(27) Ouwens, J. D.; Schropp, R. E. I.; van der Weg, W. F. *Appl. Phys. Lett.* **1994**, *65*, 204–206.

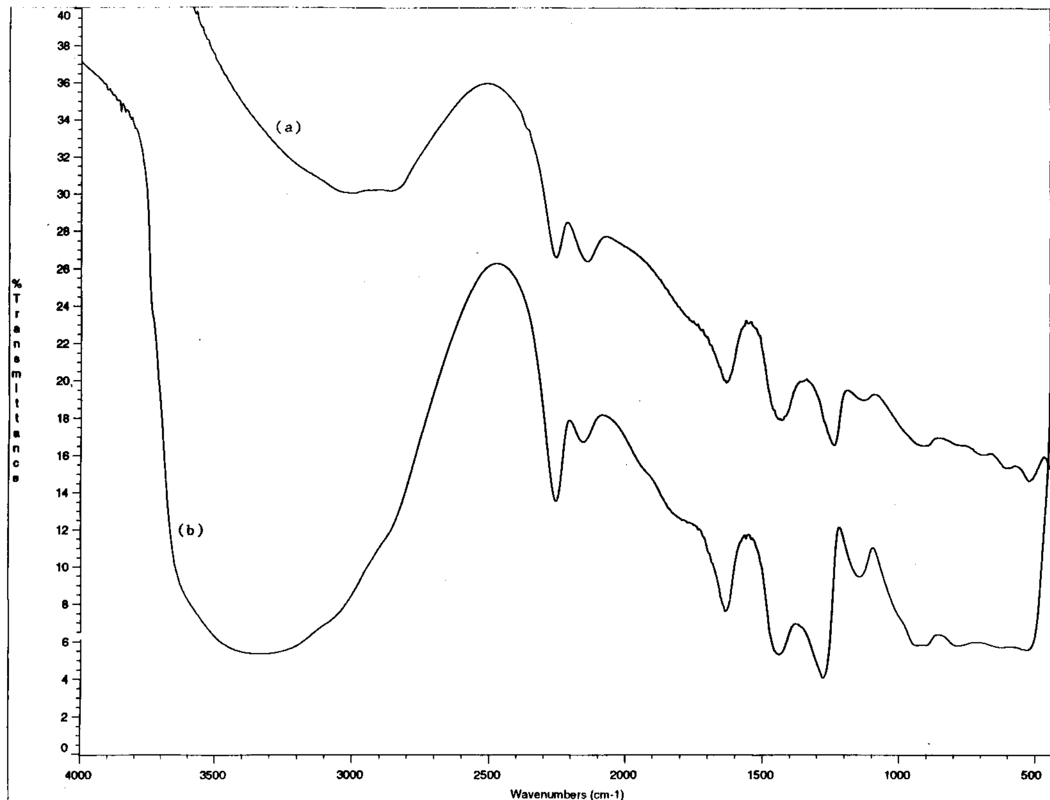

Figure 4. DRIFTS spectra for the solid product (a) before exposure to water vapor and (b) after exposure to water vapor.

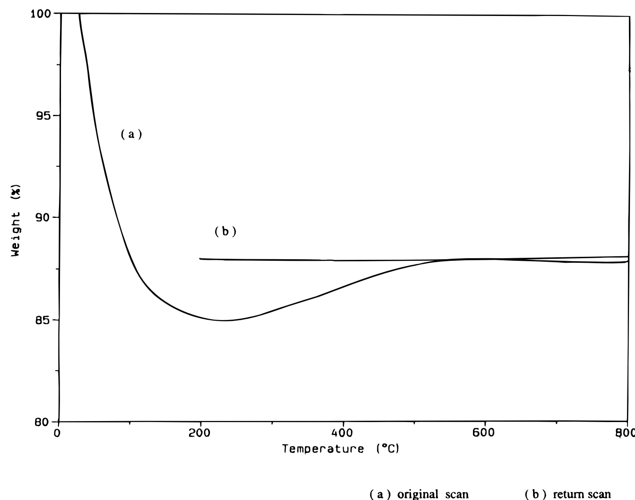

Figure 5. TGA data for solid product heated at 10 °C/min in O_2: (a) first scan; (b) return scan.

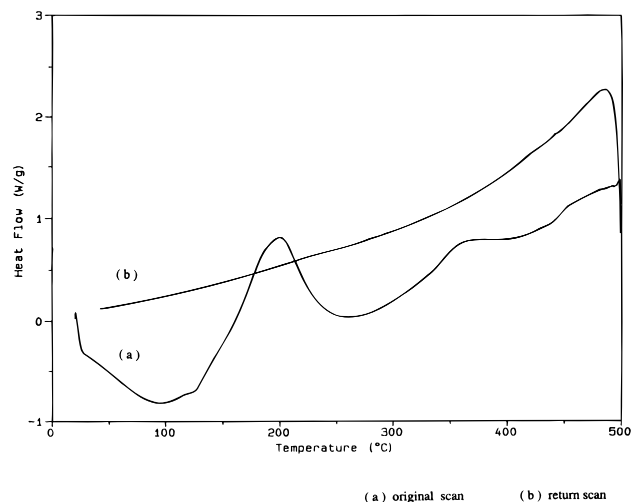

Figure 6. DSC data for solid product heated at 10 °C/min in N_2: (a) first scan; (b) return scan.

Further supporting evidence are the data of Figure 7 (vide infra).

Other surface functional groups are apparent from the SAM data of Figure 8. It is clear that Cl is present on the surface at a level of about 1%. Besides Cl at the surface, there is some carbon present probably due to adventitious carbon. Note that the level of oxygen is far below that of stoichiometric SiO_2. These data are again in line with a surface that has various functional groups including Cl and O linkages to Si.

2. Bulk Analytical Data. The energy-dispersive X-ray analyses show that the samples are primarily composed of Si. The amounts of Cl (<2%) are in good agreement with the SAM data. The XRD data of Figure 10 suggest that the material is predominantly amorphous with small amounts (~5%) of crystalline SiO_2 present.

Bulk optical properties can be obtained from the DRUV–vis data of Figure 9. From the absorption data of Figure 9, it is possible to calculate a bandgap from the absorption wavelengths for the amorphous Si material produced here. The bandgap (E_g) is between 2.4 and 2.6 eV. This value is in good agreement with E_g data for samples prepared by other methods, where E_g can vary from about 1.2 to 2.6.[19] The poor signal-to-noise ratio at low wavelengths of Figure 9 is due to poor resolution of this instrument in that region (<300 nm).

3. Thermal and Chemical Stability. The thermal stability of the amorphous Si material is consistent with

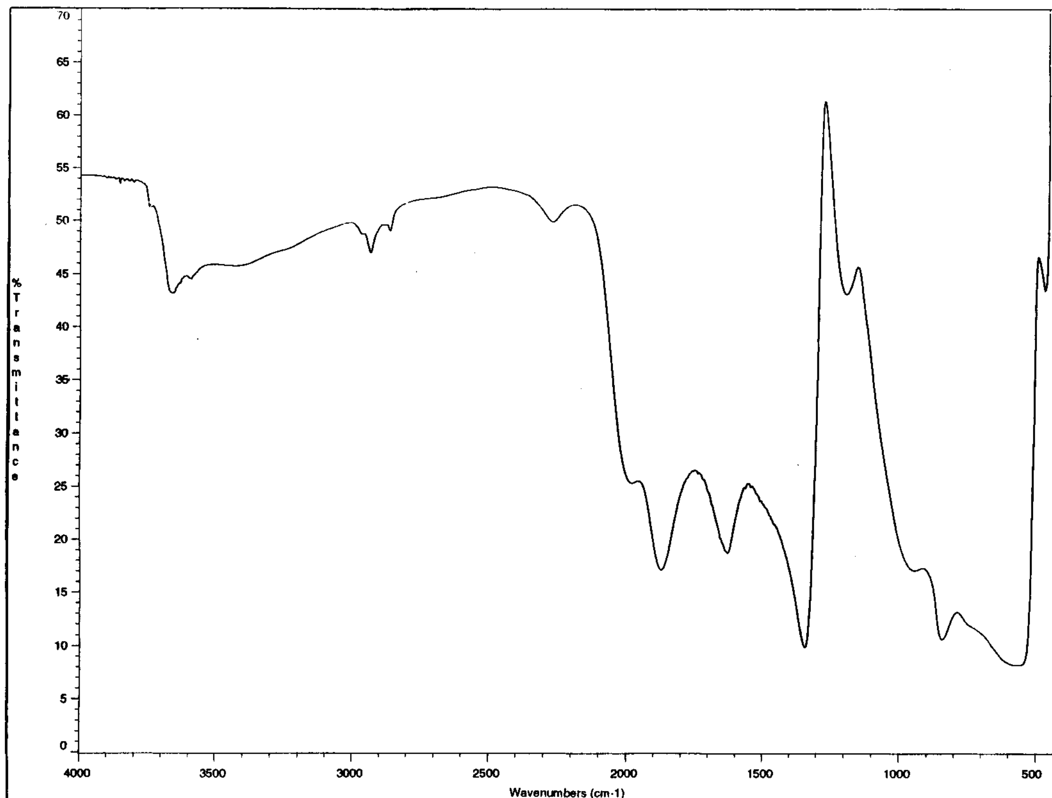

Figure 7. DRIFTS data for sample of Figure 6 after heating (after TGA).

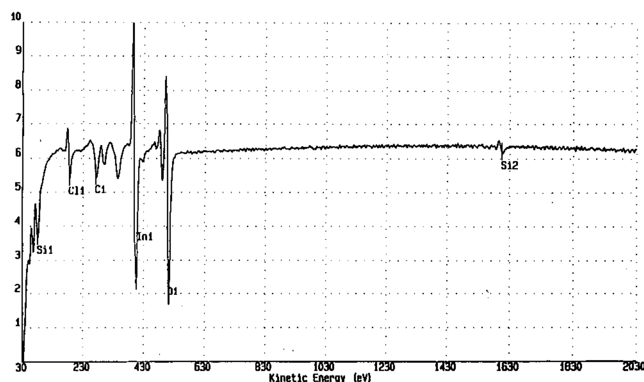

Figure 8. SAM data for the solid product.

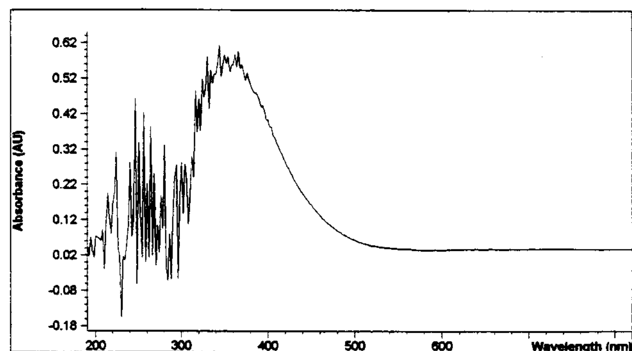

Figure 9. DRUV–vis data for the solid product.

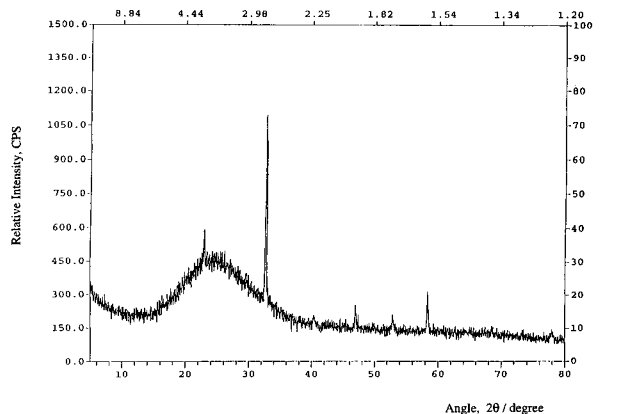

Figure 10. XRD data for the solid product.

that of published literature reports on amorphous Si.[16,20] The TGA data of Figure 5 clearly show that there is a weight gain in O_2 which is due to oxidation of the amorphous silicon. The original loss of weight is due to loss of OH groups and H from the sample. TGA data collected in N_2 gas also show a similar weight gain, although at a higher temperature, due to the lower amounts of O_2 present for oxidation.

The DSC data of Figure 6 are in accord with the above suggestion that oxidation of Si is occurring above 200 °C in an O_2 atmosphere. The exothermic nature of the oxidation of Si is a reasonable observation. The DRIFTS data of Figure 7 clearly show that OH groups are lost during the TGA process and that specific Si–OH bonds are formed on the surface as indicated by the sharp new features between 3800 and 3600 cm^{-1} and 3000 and 2800 cm^{-1}. Similar bands have been observed on silicon and silicon/aluminum containing surfaces.[21]

All of the DRIFTS, SAM, TGA, EDX, and DSC data are consistent with initial preparation of an amorphous Si phase that contains both H and Cl. This phase is chemically reactive and our spectroscopic studies suggest that the functional group changes that occur involve change from SiH_2 to SiH groups along with

generation of Si−OH groups in time on prolonged exposure to moist air or O_2.

Synthesis. The glow discharge experiments show that stable glow discharges can be obtained under H_2/He flow for prolonged periods of up to 9 h. The fact that the product can be removed from the reactor so readily is in direct contrast to similar studies that we have done using chemical vapor deposition (CVD) methods.[22] With CVD methods the adhesion of Si films to walls of the reactor is very strong and large particulates and thin-film coatings can be prepared. In the case of the ac glow discharge experiments, the particles do not adhere strongly to the surface. This may be due to the presence of the discharge, kinetic processes, the high frequency used in the experiments, and the inherent size and shape of the particulates that are formed.

The data of Figure 2 show that stable discharges can be used to prepare amorphous silicon particles. The primary reason for using ac glow discharges rather than dc discharges is to avoid the sputtering problems that occur with a dc discharge. The stability of the waveform under these conditions is interesting and suggests that major degradation of the electrodes is not occurring over at least a 9 h period.

The ac glow discharge method reported here is an inexpensive method for the preparation of amorphous silicon, in contrast to methods that typically use the more expensive SiH_4 reagent.[7,8,11] This assumes that the same quality materials can be prepared with both types of methods. The fact that little Cl is incorporated into the product is useful. Most of the Cl is trapped downstream as HCl in a cold trap. The presence of small amounts of H and Cl in amorphous Si has been suggested to be desirable[4−17,19,28−30] and can give inherent stability to such materials. The % Cl in our sample is virtually identical with desirable levels suggested by Byun et al.[29] A reviewer suggested that we look for luminescence emission in these materials. The samples do not appear to emit.

Conclusions

We have shown here that ac glow discharges can be used to prepare inorganic semiconducting materials such as amorphous silicon. The powder materials are reactive and hydrolyze in time to produce Si−OH bonds. Minor amounts of H and Cl have been incorporated into the powders. The optical properties suggest that a bandgap of 2.4−2.6 eV results. Sputtering of the electrode or wall surfaces does not seem to occur due to use of an ac glow discharge. It is likely that similar studies can be used to prepare other inorganic systems such as AlN, ZrN, TiN, SiC, Si_3N_4,[23,24] and related materials. In situ characterization studies using optical methods are the subject of ongoing research in our laboratories.[25−26,31]

Acknowledgment. We thank Fujitsu Laboratories Ltd., Hokushin Industries, Inc., and Honda R&D Co., Ltd. for support of this research. O.H.G. acknowledges the support of Colciencias, Columbia. We thank Carolina Marun, Ying Ma, Sang Hyun Park, Monica Ramos, Jeffrey A. Rozak, Z. R. Tian, X. Chen, and Dr. Y. G. Yin for help in data collection and for helpful discussions.

CM970536S

(28) Osborn, I. S.; Hata, N.; Matsuda, A. *Appl. Phys. Lett.* **1995**, *66*, 965−967.
(29) Byun, J. S.; Jeon, H. B.; Lee, K. H.; Jang, J. *Appl. Phys. Lett.* **1995**, *67*, 3786−3788.
(30) Cicala, G.; Bruno, G.; Capezutto, P. *Pure Appl. Chem.* **1996**, *68*, 1143−1149.
(31) Wiesemann, K. *Pure Appl. Chem.* **1996**, *68*, 1029−1034.